metals

MDPI

Article

Explosive Welding of Copper to High Nitrogen Austenitic Stainless Steel

Yingbin Liu [1,*], Chao Li [2], Xiaoyan Hu [1,*], Chufan Yin [1] and Tiansheng Liu [1]

[1] School of Environment and Safety Engineering, North University of China, Taiyuan 030051, China; liulang827@163.com (C.Y.); liutsh66@sina.com (T.L.)

[2] Beijing Special Vehicle Institute, Beijing 100000, China; cxlichao@163.com

* Correspondence: ybliu@nuc.edu.cn (Y.L.); huxy85@nuc.edu.cn (X.H.); Tel.: +86-1345-340-1206 (Y.L.); +86-1393-450-1236 (X.H.)

Received: 12 February 2019; Accepted: 12 March 2019; Published: 17 March 2019

Abstract: In this work, T2 red copper and high nitrogen austenitic stainless steel (HNASS) were explosively welded for the first time. The welding window was theoretically developed, and the experiment was designed by considering the effect of explosive loading on welding quality. To evaluate the welding quality, the microstructure and mechanical properties of the composite material were systematically investigated. The results showed that the welding quality was in good agreement with the results predicted by the welding window. The micromorphology of the welding interface changed with a varied welding parameter, and no intermetallic compounds were found at the welding interface by EDS analysis. The microhardness of the two raw materials both increased near the welding interface, and the enhancement increased with the explosive loading. The failure pattern of the welding interface in the tension-shear experiments was dominated by the strength failure of the red copper.

Keywords: explosive welding; copper/HNASS composite; weldability window; explosive ratio

1. Introduction

Copper/steel composite has not only the advantages of corrosion-resistance and the high toughness of copper, but also good welding capacity, formability, elongation and the thermal conductivity of steel. Therefore, copper/steel composite has received widespread attention and been used for cooling staves in the blast furnace [1].

Compared with ordinary stainless steel, high nitrogen austenite stainless steel (HNASS) containing more than 0.4% nitrogen shows excellent performances such as higher strength, wear resistance, corrosion resistance toughness, and plasticity [2]. HNASSCopper/high nitrogen steel composites will have better mechanical properties.

At present, welding technologies such as ultrasonic welding, diffusion welding, laser welding, friction welding and explosion welding are applied to prepare dissimilar metal composites. Compared with other welding methods, explosive welding is a better choice for manufacturing composites with large areas.

Explosive welding is a one of the solid method which forms metallurgical bonding between metals by using the energy released by an explosive. It is not only an important method for connecting the metal parts, but also a basic synthetic technology of metal materials. A variety of metallic composite plates have been manufactured by the explosive welding method. Lazurenko et al. [3] discussed the explosive welding window of the AISI 304 stainless steel/6082-T6 aluminum alloy composite and proved that the position of materials influenced the weldability. Zhang et al. [1] successfully obtained copper-steel composite by explosive welding and investigated the microstructure and mechanical

properties of the copper-steel composite. The interface presented a periodic wavy pattern, and a transition layer could be found after heat treatment. Bina et al. [4] studied the effect of the heat treatment time on the bonding interface and the mechanical properties of copper-stainless steel composite produced by explosive welding. Miao et al. [5] obtained two composite plates simultaneously through one explosion. Athar and Tolaminejad [6] calculated the weldability window of aluminum-copper and studied the influence of welding parameters on the interface morphology and the mechanical properties of Al/Cu/Al composites. The interface morphology and the mechanical properties were different under different conditions of explosive welding. Mousavi and Sartangi [7] calculated the weldability domain for explosive welding of cp-titanium to AISI 304 stainless steel and investigated the effect of different welding parameters on microstructure of interfaces. Durgutlu et al. [8] demonstrated that the stand-off distance influenced the microstructure and the hardness of the interface.

Generally, the Vickers hardness of ordinary stainless steel is about 200HV, and the tensile strength is about 520 MPa. The Vickers hardness and tensile strength of HNASS are about 350 HV and 1200 MPa, respectively. Thus, the explosion parameters used for explosive welding of copper and stainless steel are not suitable for explosive welding of copper/HNASS.

In this paper, the explosive welding window of the copper/HNASS composites was calculated. On this basis, the copper/HNASS composite plates were prepared through the explosive welding approach. The effect of the explosive welding parameters on the microstructure and the mechanical properties of the copper/HNASS composite after welding were studied.

2. Weldability Window Calculations

According to the theory and practice of explosive welding, the welding parameters need to meet an appropriate range to obtain a good welding quality for each kind of metal combination, which is called weldability window or standard. Cowan et al. [9] put forward a weldability standard according to the mechanical properties of the flyer and parent plate materials. However, Mousavi and Al-Hassani [10] believed that the welding effect obtained according to the standard was not satisfactory. Later Carpenter [11] and Deribas [12] proposed a more practical weldability window (see Figure 1), which was the function of the collision point velocity V_c, and the collision angle β.

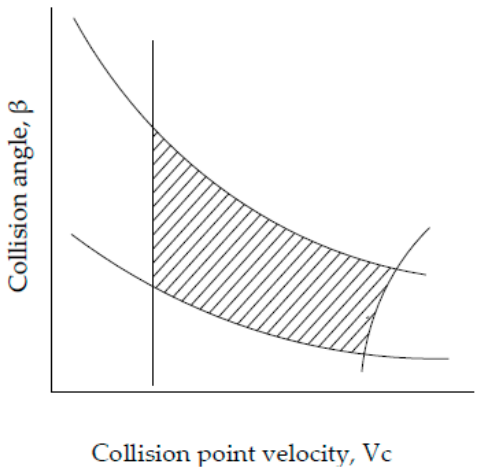

Figure 1. Weldability window for explosive welding.

As seen from Figure 1, the weldability window is composed of four boundaries. The flyer plate and base plate were welded by the high-speed collision of plane or small angle during the explosive welding process [13]. The research indicated that a firm bonding could be formed between metals when the plastic deformation on the contact surface was fully developed and the jet was formed. This condition is limited by the lower boundary of the welding zone on the β–V_c coordinate plane. Therefore, the lower boundary of the explosive welding can be defined to meet the condition that the

impact pressure at the collision point should be greater than the yield stress of the material to produce the plastic deformation of the welding material. Zakharenko and Zlobin [14] considered that the collision angle β is determined by the Vickers Hardness H_V, the density ρ, the minimum collision point velocity V_c and a constant k_1 (see Equation (1)). When the difference between the material properties is smaller, H_V is the Vickers Hardness of the flyer plate. When the properties of welded materials are very different, H_V is the average Vickers hardness of two welded materials [15]. The density ρ is the density of the flyer plate material. Specifically, the constant k_1 ranges from 0.6 to 1.2 [16]. When the metal surface is well pre-processed, the constant k_1 can be taken as 0.6.

$$\beta = \frac{k_1}{V_c}\left(\frac{H_V}{\rho}\right)^{\frac{1}{2}} \tag{1}$$

For the same purpose, Belayev et al., as mentioned by Lysak and Kuzmin [17], developed another equation to calculate the collision angle

$$\beta = 1.8\left[\frac{1}{V_c}\sqrt{\frac{\sigma_b}{\rho}} + 0.1\left(\frac{V_c}{C_b + 1550}\right)^2\right] \tag{2}$$

where σ_b and C_b are the tensile strength and the bulk sound velocity of the flyer plate, respectively.

The upper limit of this area represents the maximum collision speed between the flyer and parent plate, that is, the maximum load in explosive welding. If the collision speed is above this line, a failure weld will occur because of the excessive melting of the joint surface. Zheng [13] mentioned that Wittman derived the equation for maximum collision speed V_p (see Equation (3)) from the thermal effect of the joint area. The calculating formula of the collision angle β can be established by using Equation (4). T_m is the melting temperature of the material, K is the heat conduction coefficient, C_p is the specific heat at constant pressure, t_f is the thickness of the flyer plate, N is the dimensional constant taking a value of 0.11 for several metals according to Rosset [18].

$$V_p = \frac{1}{N}\frac{(T_m C_b)^{\frac{1}{2}}}{V_c}\left(\frac{KC_pC_b}{\rho t_f}\right)^{\frac{1}{4}} \tag{3}$$

$$\sin\left(\frac{\beta}{2}\right) = \frac{V_p}{2V_c} = \frac{1}{2N}\frac{(T_m C_b)^{\frac{1}{2}}}{V_c^2}\left(\frac{KC_pC_b}{\rho t_f}\right)^{\frac{1}{4}} \tag{4}$$

In order to calculate the upper boundary, however, Deribas [15] derived a different equation (see Equation (5)) by connecting the kinematic parameters with the thermal physical and geometric parameters of colliding materials. Where t_p is the thickness of the parent plate, others are the same as before.

$$\sin\frac{\beta}{2} = 14.7V_c^{-\frac{5}{4}}\sqrt{\frac{T_m K/a}{\rho t_f^{\frac{1}{2}} t_p/\left(t_f + t_p\right)}} \tag{5}$$

$$a = \sqrt{K/\left(\rho C_p\right)} \tag{6}$$

The right limit of the weldability window is the consequence of formation of a jet [13]. The collision point velocity V_c in this case is the critical velocity of the jet of formation. In order to satisfy this condition, Walsh, et al. [19] considered that V_c should be smaller than the C_b (see Equation (7)) of the welded materials.

$$V_c < C_b \tag{7}$$

In the explosion welding process, good wave joints usually obtain a high bonding strength. When the collision point velocity V_c is smaller than a certain value, the bonding area is a linear interface

instead of a wavy interface. The certain value is defined as the transition velocity from turbulent to laminar flow and is the leftmost line of the weldability window. Cowan, Bergmann and Holtzman [9] pointed out that the speed depended on the properties of the metals to be welded. According to the fluid dynamics theory, the collision point velocity V_c could be described as a function of the hardness and density of two metals (see Equation (8)).

$$V_c = \sqrt{\frac{2\mathrm{Re}\left(H_{V,p} + H_{V,f}\right)}{\rho_p + \rho_f}} \tag{8}$$

When the explosive welding configuration is asymmetric, the Reynolds number Re is about 8.0~13.0, ρ_f and ρ_p are respectively the density of the flyer and parent plate, $H_{V,p}$ and $H_{V,f}$ are their Vickers hardness.

The T2 red copper and HNASS were used as the flyer and base plate materials in this work, respectively. The physical and mechanical parameters related to the welding materials are shown in Table 1. The weldability window of the T2 red copper and HNASS was calculated using Equations (1)–(8) (see Figure 2).

Table 1. Physical and mechanical parameters related to the welding materials used in this study.

Materials	ρ ($\mathrm{g{\cdot}cm^{-3}}$)	H_v (HV)	σ_b (MPa)	C_b (m/s)	T_m (K)	K ($\mathrm{W{\cdot}m^{-1}{\cdot}K^{-1}}$)	C_p ($\mathrm{J{\cdot}kg^{-1}{\cdot}K^{-1}}$)
T2 red copper	8.93	56	232	4730	1135	402	381
HNASS	7.82	320	1130	4600	1725	17	470

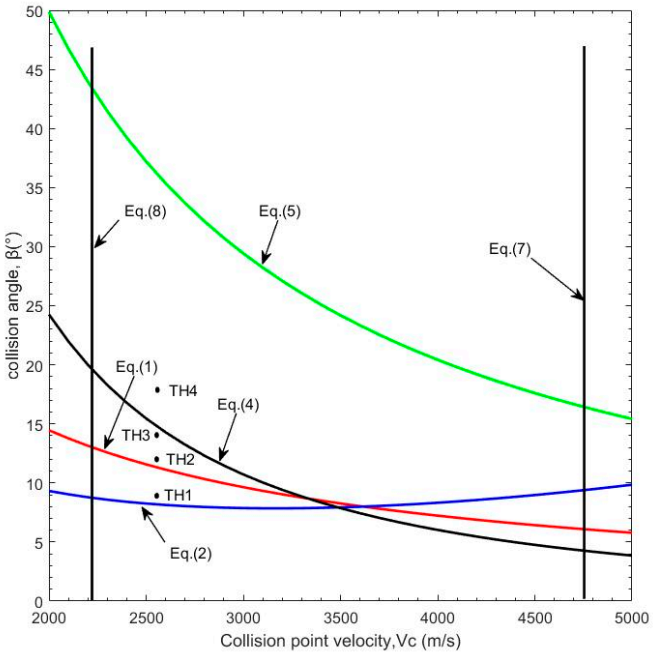

Figure 2. The explosive welding weldability window for the red copper and HNASS calculated using Equations (1)–(8).

3. Materials and Methods

The chemical composition of T2 red copper and HNASS are given in Table 2. The dimensions of T2 red copper and HNASS are 200 × 40 × 2 $\mathrm{mm^3}$ and 200 × 40 × 5 $\mathrm{mm^3}$. The parallel welding technique was adopted in this study. The distance between the two plates was 6 mm. The explosive used was rock ammonium nitrate. The density was 0.8 $\mathrm{g/cm^3}$ and the detonation velocity was measured to be

~2550 m/s. The explosive welding device is shown in Figure 3. In the case of the parallel welding technique and using nitroamine explosives, the relation between the Impact velocity (V_p), the explosive ratio and the detonation velocity was expressed as [15]

$$V_p = 1.2V_d\left[\frac{\left(1+\frac{32}{27}R\right)^{\frac{1}{2}}-1}{\left(1+\frac{32}{27}R\right)^{\frac{1}{2}}+1}\right] = 2V_d\sin\left(\frac{\beta}{2}\right) \quad (9)$$

Table 2. Chemical composition of T2 red copper and HNASS (wt %).

Element Name	N	C	Mn	Ni	Cr	Mo	Cu	W	Fe	Sb	Bi	As	Pb	S
T2 red copper	–	–	–	–	–	–	Bal.	–	0.005	0.002	0.001	0.002	0.005	0.005
HNASS	0.88	0.03	19.28	2.01	19.32	0.0001	0.031	0.005	Bal.	–	–	–	–	–

Figure 3. Explosive welding device.

R is the ratio of mass of explosive to the mass of the flyer plate per unit area. According to the calculation results of the welding window, different explosive welding parameters (see Table 3) were selected for welding experiment respectively.

Table 3. Explosive welding parameters for different welding experiment.

Number	Stand-off Distance (mm)	Detonation Velocity (m/s)	Impact Velocity (m/s)	Collision Angle β (°)	Explosive Ratio R	Charge Depth (mm)
TH-1	6	2550	400	9	0.6	13
TH-2	6	2550	533	12	0.9	20
TH-3	6	2550	622	14	1.1	24
TH-4	6	2550	798	18	1.6	36

In order to obtain an insight view on the welding interfaces, the specimens with the dimension of $15 \times 10 \times 7$ mm^3 were draw out along the detonation direction. The specimens were orderly ground using the sandpapers of W50, W28, W14, W7 and W3.5 respectively. Finally, they were polished with 1.5 μm diamond polishing powder and etched. And the microstructure of the sample was observed with an Axio Lab. A1 optical microscope (Carl Zeiss, Oberkochen, Germany). The distribution of metallic elements across the bonding interface under different conditions was analyzed using Energy-dispersive X-ray spectroscopy (EDS Inca X-Max, Oxford instruments, Oxford, UK).

Measurements on the microhardness of the parent materials close to the welding interface were carried out by Huayin HV-1000A vickers hardness instrument (Huayin test instrument Co. LTD, Wuhan, China) with 300 g load for 10 s. At the same time, the tension-shear tests were conducted using a GB/T 6396-2008 materials test system. The dimensions of the tensile specimen are shown in Figure 4, and the samples were cut along with the detonation direction.

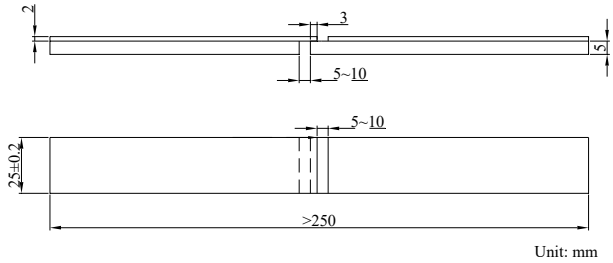

Figure 4. Dimensions of the tensile specimen.

4. Results and Discussion

From the observation of the welding interfaces, the composite was not successfully welded for the explosive ratio R = 0.6. However, composites obtained by using other explosive welding parameters were successfully welded. As shown in Figure 2, for R = 0.6, the point was located over the lower boundary calculated by Equation (2), but below the lower boundary calculated by Equation (1). For R = 0.9, the point is situated in the upper of the boundary calculated by Equation (1), the composite was successfully welded. Therefore, for the explosive welding of T2 red copper/HNASS, the lower boundary can calculate using Equation (1) and consider the hardness of HNASS.

4.1. Morphology of the Joint Surface

The morphologies of the bonding interface using different welding parameters are shown in Figure 5. It can be observed that the bonding interface is different for different parameters. As can be seen from Figure 5a, a relative flat joint interface without obvious regular oscillations can be observed in TH-2. The morphology of the interface is similar to that of Al/Cu composite as indicated by Loureiro, et al. [20]. However, the joint surface presents a regular wave bonding pattern in TH-3 (see Figure 5b) and the wavelength is about 200 μm. The wavelength and the amplitude of the bonding interface gradually increase with increasing ratio of the explosive. For TH-4 (see Figure 5c), the wavelength of the bonding interface is about 150 μm. Nevertheless, several copper melts and thin HNASS strips penetrated into the T2 red copper plate at the joint interface.

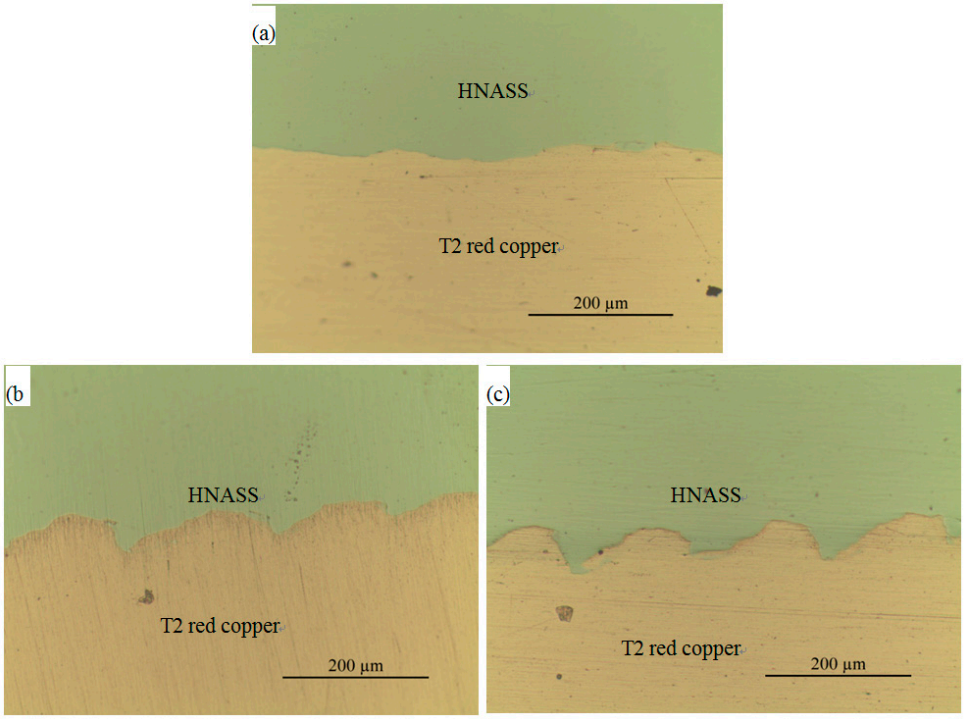

Figure 5. Morphologies of the joint surface for different explosive ratios. (**a**) *R*=0.9; (**b**) *R*=1.1; (**c**) *R*=1.6.

The grains of the T2 red copper closing to the welding interface are shown in Figure 6. As shown, the grains of the T2 red copper in all composite samples were refined and elongated along the detonation direction. This should be attributed to the plastic deformation generated by the high-velocity collision between the flyer plate and the parent plate. Meanwhile, it was observed that the numbers of the refined grains and the grain refinement both increase with increasing explosive ratio.

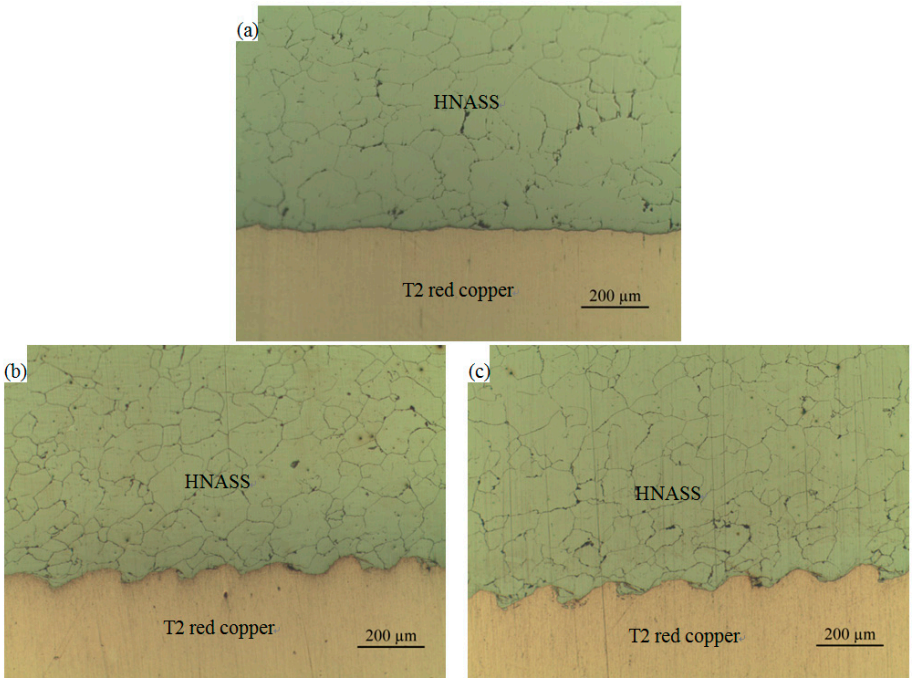

Figure 6. Grains of the parent plate near the joint interface for different explosive ratios. (**a**) *R* = 0.9; (**b**) *R* = 1.1; (**c**) *R* = 1.6.

In general, the energy of the detonation wave and the detonation products is instantaneously transmitted to the flyer plate, accelerating the flyer plate to a high velocity. The flyer plate impacted on the parent plate, generating high temperature and high pressure at the interface, thus bonding the plates together. The formation of the explosive welding joint is the process of plastic deformation of a thin layer of metal on the interface under explosive loading; the closer to the interface, the greater the plastic deformation. During this process, part of the energy of the explosive is converted into the plastic deformation energy of the metal in the joint area. Then, the plastic (shear) energy is converted into heat energy by means of the plastic deformation process, which causes the plastic deformed metal close to the interface to melt. The impact velocity and pressure of the plates increase with the increase of the explosive ratio, leading to higher impact energy and work of plastic (shear) deformation during the collision. When the explosive ratio is small, the energy produced by the explosive is not enough to cause plastic deformation of HNASS, resulting in the failure of explosive welding or the appearance of linear interface. If the explosive ratio is relatively large, the energy produced by the explosive will not only form good bonding between the flyer plate and the parent plate, but also cause metals near the joint interface to melt.

4.2. EDS Analysis

Figure 7 shows the element line scanning near the joint surface under different explosive welding conditions. As can be seen from the figure, although the bonding interface is different under different explosive welding conditions, no intermetallic compounds are generated near the joint interface under the three conditions. Although some copper melts near the interface when R = 1.6, in this case the power generated from the explosive is not enough to produce intermetallic compound at the interface. The formation of intermetallic compound could reduce the bonding strength of the two metals. Therefore, the bonding strength of composites under the three conditions will not be affected by the intermetallic compound.

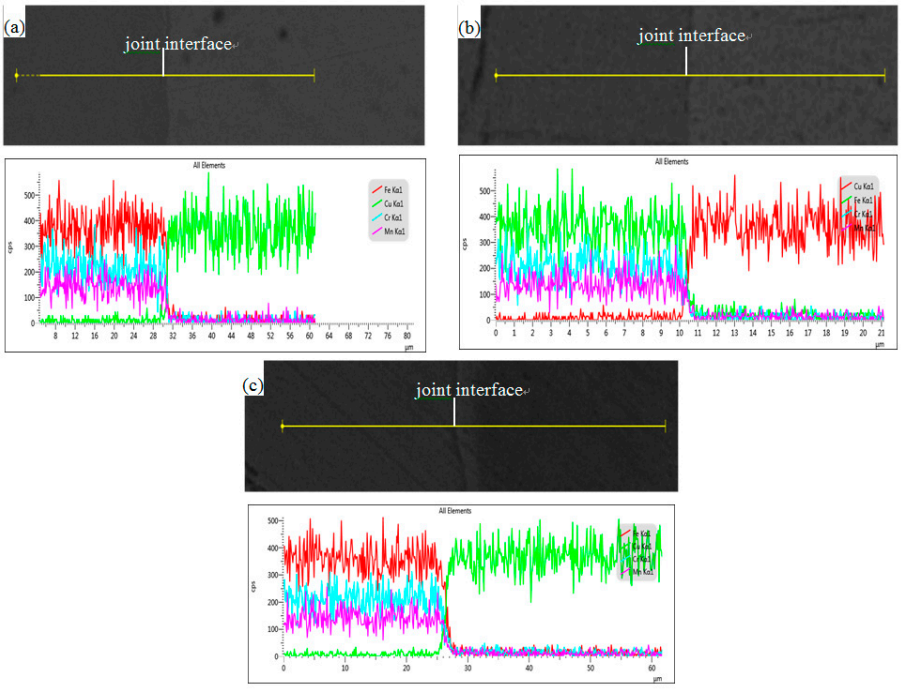

Figure 7. Element line scanning near the joint surface under different explosive welding conditions. (**a**) R = 0.9; (**b**) R = 1.1; (**c**) R = 1.6.

4.3. Microhardness

The measured results of the microhardness for different explosive welding parameters are shown in Figure 8. It can be observed that the microhardness value at the joint surface of the sample after explosive welding is the highest. On each side of the bonding interface, the microhardness value decreases gradually and then becomes stable as the distance from the bonding interface increases. This is mainly because of the plastic deformation near the joint interface which occurs when two plates collide with each other at high speed during explosive welding. The plastic deformation causes strain hardening of the material, which improves the hardness of the material; the closer to the joint interface, the more serious the plastic deformation. When the distance from the interface exceeds a certain distance, no plastic deformation occurs. This phenomenon is consistent with the previous research demonstrated by Kacar and Acarer [21]. By comparing the microhardness values under different welding conditions, the larger the explosive ratio, the higher the microhardness value at the joint interface, indicating the greater the degree of hardening at both sides of the joint surface. This is mainly because that the larger the explosive ratio, the higher the collision speed of two plates, which leading to greater impact pressure and plastic deformation during the collision process. As already mentioned, there is plastic deformation near the interface. The microhardness value increases with the increase of plastic deformation degree.

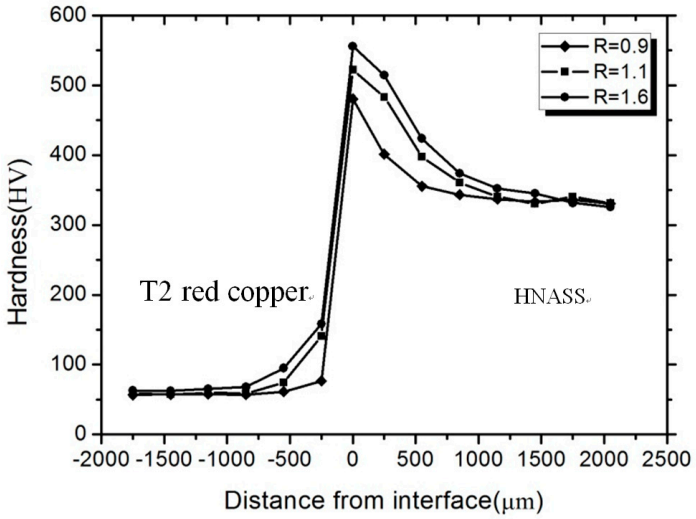

Figure 8. Microhardness values of T2 red copper/HNASS under different explosive welding parameter.

4.4. Tensile Shear Test Result

Tensile shear tests were carried out for explosive welding samples under different conditions. For all specimens, the fracture occurred on T2 red copper plate. The test results of tensile shear are shown in the Table 4. It can be clearly found from the results that all the results are greater than 230 MPa, indicating that T2 red copper has been strengthened after explosive welding. For R = 0.9 which the joint surface presents linear-like morphology, the tensile strength is 258 MPa. For the two cases (R = 1.1 and 1.6) which the joint surface present regular wave bonding, the tensile strength of the sample is 295 MPa and 310 MPa respectively. This indicates that as the ratio of explosive increases, the tensile strength of the sample increases, and the enhancement degree of T2 red copper is different under different explosive ratio. This is also because of grain refinement near the binding domain, which is consistent with the grain refinement of high-nitrogen steel after explosive welding observed above.

Table 4. Test results of tensile shear of T2 red copper/HNASS under different explosive welding parameters.

Explosive Ratios	R = 0.9	R = 1.1	R = 1.6
Tensile strength (MPa)	258	295	310
Ruptured material	T2 red copper	T2 red copper	T2 red copper

In general, the bonding strength of composites with linear-like interface is slightly lower than that of the wavy interface obtained under higher explosive ratio. But, the tensile strength of copper with linear-like interface was 258 MPa, which is higher than the strength of T2 red copper, and the joint surface was not separated, indicating that the bonding quality obtained in this case was safe. This is consistent with the earlier work [22].

5. Conclusions

The weldability window of T2 red copper/HNASS was calculated. On this basis, T2 red copper/HNASS composites were manufactured by explosive welding using different explosive welding parameters, and the microstructure and mechanical properties of T2 red copper/HNASS composites explosive welded were studied. The following conclusions can be drawn:

1. A T2 red copper/HNASS composite could be successfully obtained by the explosive welding method if the proper explosive welding parameters were adopted, and the lower boundary should be calculated considering the mechanical parameters of HNASS.
2. The morphology of the joint surface is different under different explosive welding parameters, and regular wave bonding can occur for larger explosive ratio.
3. Although the joint interface was different under different explosive welding conditions, no intermetallic compounds were generated near the joint interface under three conditions.

Author Contributions: Data curation, Y.L. and C.Y.; Formal analysis, X.H.; Investigation, Y.L. and X.H.; Methodology, C.L.; Resources, T.L.; Supervision, T.L.; Writing—original draft, Y.L.

Funding: This research was funded by the National Nature Science of China (No. 11802274 and No. 11572292) and Open Research Fund of Key Laboratory of North University of China (No. DXMBJJ2018-01).

Conflicts of Interest: The authors declare no conflict of interest.

References

1. Zhang, H.; Jiao, K.X.; Zhang, J.L.; Li, J. Microstructure and mechanical properties investigations of copper-steel composite fabricated by explosive welding. *Mater. Sci. Eng. A Struct. Mater. Prop. Microstruct. Process.* **2018**, *731*, 278–287. [CrossRef]
2. Shi, F.; Cui, W.; Wang, L.; Jiang, Z.; Liu, C. Advance in the research of high-nitrogen austenitic stainless steels. *Shanghai Met.* **2006**, *28*, 45–50. (In Chinese)
3. Lazurenko, D.V.; Bataev, I.A.; Mali, V.I.; Jorge, A.M., Jr.; Stark, A.; Pyczak, F.; Ogneva, T.S.; Maliutina, I.N. Synthesis of metal-intermetallic laminate (mil) composites with modified al3ti structure and in situ synchrotron x-ray diffraction analysis of sintering process. *Mater. Des.* **2018**, *151*, 8–16. [CrossRef]
4. Bina, M.H.; Dehghani, F.; Salimi, M. Effect of heat treatment on bonding interface in explosive welded copper/stainless steel. *Mater. Des.* **2013**, *45*, 504–509. [CrossRef]
5. Miao, G.; Ma, H.; Shen, Z.; Yu, Y. Research on honeycomb structure explosives and double sided explosive cladding. *Mater. Des.* **2014**, *63*, 538–543. [CrossRef]
6. Athar, M.M.H.; Tolaminejad, B. Weldability window and the effect of interface morphology on the properties of al/cu/al laminated composites fabricated by explosive welding. *Mater. Des.* **2015**, *86*, 516–525. [CrossRef]
7. Mousavi, S.A.A.A.; Sartangi, P.F. Experimental investigation of explosive welding of cp-titanium/aisi 304 stainless steel. *Mater. Des.* **2009**, *30*, 459–468. [CrossRef]
8. Durgutlu, A.; Okuyucu, H.; Gulenc, B. Investigation of effect of the stand-off distance on interface characteristics of explosively welded copper and stainless steel. *Mater. Des.* **2008**, *29*, 1480–1484. [CrossRef]

9. Cowan, G.R.; Bergmann, O.R.; Holtzman, A.H. Mechanism of bond zone wave formation in explosion-clad metals. *Metall. Mater. Trans. B* **1971**, *2*, 3145–3155. [CrossRef]
10. Mousavi, A.A.A.; Al-Hassani, S.T.S. Numerical and experimental studies of the mechanism of the wavy interface formations in explosive/impact welding. *J. Mech. Phys. Solids* **2005**, *53*, 2501–2528.
11. Carpenter, S.H.; Wittman, R.H. Explosion welding. *Ann. Rev. Mater. Res.* **1975**, *5*, 177–199. [CrossRef]
12. Deribas, A. *Physics of Hardening and Welding by Explosion*; Nauka: Novosibirsk, Russia, 1972.
13. Zheng, Z. *Explosive Working*; National Defense Industry Press: Beijing, China, 1981.
14. Zakharenko, I.D.; Zlobin, B.S. Effect of the hardness of welded materials on the position of the lower limit of explosive welding. *Combust. Explos. Shock Waves* **1983**, *19*, 689–692. [CrossRef]
15. Sun, T.-E.C. *Explosion Physics*; Science Press: Beijing, China, 2011.
16. Zamani, E.; Liaghat, G.H. Explosive welding of stainless steel–carbon steel coaxial pipes. *J. Mater. Sci.* **2012**, *47*, 685–695. [CrossRef]
17. Lysak, V.I.; Kuzmin, S.V. Lower boundary in metal explosive welding. Evolution of ideas. *J. Mater. Process. Technol.* **2012**, *212*, 150–156. [CrossRef]
18. de Rosset, W.S. Analysis of explosive bonding parameters. *Mater. Manuf. Process.* **2006**, *21*, 634–638. [CrossRef]
19. Walsh, J.M.; Shreffler, R.G.; Willig, F.J. Limiting conditions for jet formation in high velocity collisions. *J. Appl. Phys.* **1953**, *24*, 349–359. [CrossRef]
20. Loureiro, A.; Mendes, R.; Ribeiro, J.B.; Leal, R.M.; Galvao, I. Effect of explosive mixture on quality of explosive welds of copper to aluminium. *Mater. Des.* **2016**, *95*, 256–267. [CrossRef]
21. Kacar, R.; Acarer, M. An investigation on the explosive cladding of 316l stainless steel-din-p355gh steel. *J. Mater. Process. Technol.* **2004**, *152*, 91–96. [CrossRef]
22. Kaya, Y.; Kahraman, N. An investigation into the explosive welding/cladding of grade a ship steel/aisi 316l austenitic stainless steel. *Mater. Des.* **2013**, *52*, 367–372. [CrossRef]